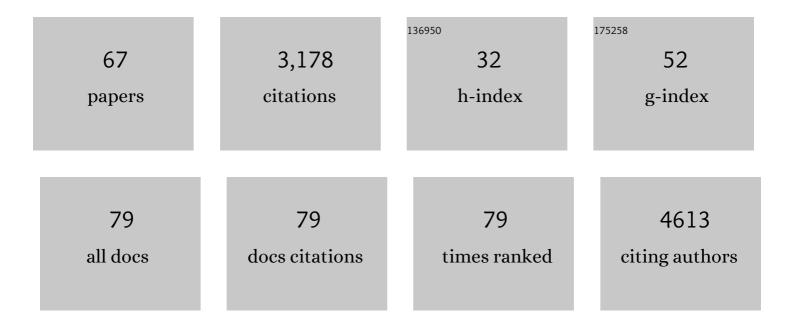
Siawoosh Mohammadi

List of Publications by Year in descending order

Source: https://exaly.com/author-pdf/7808904/publications.pdf Version: 2024-02-01



#	Article	IF	CITATIONS
1	Serum C-reactive protein is linked to cerebral microstructural integrity and cognitive function. Neurology, 2010, 74, 1022-1029.	1.1	196
2	Advances in MRI-based computational neuroanatomy. Current Opinion in Neurology, 2015, 28, 313-322.	3.6	166
3	hMRI – A toolbox for quantitative MRI in neuroscience and clinical research. NeuroImage, 2019, 194, 191-210.	4.2	161
4	Correcting eddy current and motion effects by affine wholeâ€brain registrations: Evaluation of threeâ€dimensional distortions and comparison with slicewise correction. Magnetic Resonance in Medicine, 2010, 64, 1047-1056.	3.0	129
5	Nerve fiber impairment of anterior thalamocortical circuitry in juvenile myoclonic epilepsy. Neurology, 2008, 71, 1981-1985.	1.1	126
6	Traumatic and nontraumatic spinal cord injury: pathological insights from neuroimaging. Nature Reviews Neurology, 2019, 15, 718-731.	10.1	125
7	Sex-Dependent Influences of Obesity on Cerebral White Matter Investigated by Diffusion-Tensor Imaging. PLoS ONE, 2011, 6, e18544.	2.5	121
8	Quantitative magnetic resonance imaging of brain anatomy and in vivo histology. Nature Reviews Physics, 2021, 3, 570-588.	26.6	115
9	Microstructural imaging of human neocortex in vivo. NeuroImage, 2018, 182, 184-206.	4.2	101
10	Whole-Brain In-vivo Measurements of the Axonal G-Ratio in a Group of 37 Healthy Volunteers. Frontiers in Neuroscience, 2015, 9, 441.	2.8	97
11	Integrity of the hippocampus and surrounding white matter is correlated with language training success in aphasia. Neurolmage, 2010, 53, 283-290.	4.2	93
12	A general linear relaxometry model of R ₁ using imaging data. Magnetic Resonance in Medicine, 2015, 73, 1309-1314.	3.0	90
13	Volume Estimation of the Thalamus Using Freesurfer and Stereology: Consistency between Methods. Neuroinformatics, 2012, 10, 341-350.	2.8	77
14	Microstructural and volumetric abnormalities of the putamen in juvenile myoclonic epilepsy. Epilepsia, 2011, 52, 1715-1724.	5.1	76
15	Estimating the apparent transverse relaxation time (R2*) from images with different contrasts (ESTATICS) reduces motion artifacts. Frontiers in Neuroscience, 2014, 8, 278.	2.8	68
16	Local but not long-range microstructural differences of the ventral temporal cortex in developmental prosopagnosia. Neuropsychologia, 2015, 78, 195-206.	1.6	67
17	Can the Language-dominant Hemisphere Be Predicted by Brain Anatomy?. Journal of Cognitive Neuroscience, 2011, 23, 2013-2029.	2.3	61
18	The impact of post-processing on spinal cord diffusion tensor imaging. Neurolmage, 2013, 70, 377-385.	4.2	59

#	Article	IF	CITATIONS
19	NODDI-DTI: Estimating Neurite Orientation and Dispersion Parameters from a Diffusion Tensor in Healthy White Matter. Frontiers in Neuroscience, 2017, 11, 720.	2.8	54
20	Voxel-based analysis of grey and white matter degeneration in cervical spondylotic myelopathy. Scientific Reports, 2016, 6, 24636.	3.3	52
21	Early microstructural white matter changes in patients with HIV: A diffusion tensor imaging study. BMC Neurology, 2012, 12, 23.	1.8	51
22	DIFFUSION TENSOR IMAGING DEMONSTRATES FIBER IMPAIRMENT IN SUSAC SYNDROME. Neurology, 2008, 70, 1867-1869.	1.1	50
23	Diffusion-Tensor Imaging at 3 T. Investigative Radiology, 2007, 42, 338-345.	6.2	49
24	Dorsal and ventral horn atrophy is associated with clinical outcome after spinal cord injury. Neurology, 2018, 90, e1510-e1522.	1.1	44
25	Correction of vibration artifacts in DTI using phaseâ€encoding reversal (COVIPER). Magnetic Resonance in Medicine, 2012, 68, 882-889.	3.0	40
26	Towards in vivo g-ratio mapping using MRI: Unifying myelin and diffusion imaging. Journal of Neuroscience Methods, 2021, 348, 108990.	2.5	40
27	G-CSF Prevents the Progression of Structural Disintegration of White Matter Tracts in Amyotrophic Lateral Sclerosis: A Pilot Trial. PLoS ONE, 2011, 6, e17770.	2.5	39
28	Embodied neurology: an integrative framework for neurological disorders. Brain, 2016, 139, 1855-1861.	7.6	39
29	Specific pattern of early whiteâ€matter changes in pure hereditary spastic paraplegia. Movement Disorders, 2010, 25, 1986-1992.	3.9	37
30	Adaptive smoothing of multi-shell diffusion weighted magnetic resonance data by msPOAS. NeuroImage, 2014, 95, 90-105.	4.2	36
31	The Influence of Spatial Registration on Detection of Cerebral Asymmetries Using Voxel-Based Statistics of Fractional Anisotropy Images and TBSS. PLoS ONE, 2012, 7, e36851.	2.5	36
32	Gelastic seizures: A case of lateral frontal lobe epilepsy and review of the literature. Epilepsy and Behavior, 2009, 15, 249-253.	1.7	35
33	Four in vivo <i>g</i> â€ratioâ€weighted imaging methods: Comparability and repeatability at the group level. Human Brain Mapping, 2018, 39, 24-41.	3.6	34
34	The effect of local perturbation fields on human DTI: Characterisation, measurement and correction. NeuroImage, 2012, 60, 562-570.	4.2	33
35	Vascular autorescaling of fMRI (VasA fMRI) improves sensitivity of population studies: A pilot study. NeuroImage, 2016, 124, 794-805.	4.2	33
36	Dynamic changes in white matter microstructure in anorexia nervosa: findings from a longitudinal study. Psychological Medicine, 2019, 49, 1555-1564.	4.5	33

#	Article	IF	CITATIONS
37	Retrospective correction of physiological noise in DTI using an extended tensor model and peripheral measurements. Magnetic Resonance in Medicine, 2013, 70, 358-369.	3.0	32
38	Voxelâ€Based Statistical Analysis of Fractional Anisotropy and Mean Diffusivity in Patients with Unilateral Temporal Lobe Epilepsy of Unknown Cause. Journal of Neuroimaging, 2013, 23, 352-359.	2.0	31
39	Neurodegeneration in the Spinal Ventral Horn Prior to Motor Impairment in Cervical Spondylotic Myelopathy. Journal of Neurotrauma, 2017, 34, 2329-2334.	3.4	30
40	In vivo evidence of remote neural degeneration in the lumbar enlargement after cervical injury. Neurology, 2019, 92, e1367-e1377.	1.1	29
41	Transient lesion in the splenium related to antiepileptic drug: Case report and new pathophysiological insights. Seizure: the Journal of the British Epilepsy Association, 2008, 17, 654-657.	2.0	25
42	A novel splice site mutation in the <i>SPG7</i> gene causing widespread fiber damage in homozygous and heterozygous subjects. Movement Disorders, 2010, 25, 413-420.	3.9	25
43	Synthetic quantitative MRI through relaxometry modelling. NMR in Biomedicine, 2016, 29, 1729-1738.	2.8	25
44	The efficiency of retrospective artifact correction methods in improving the statistical power of between-group differences in spinal cord DTI. NeuroImage, 2017, 158, 296-307.	4.2	25
45	Neuroimaging in Susac's syndrome: Focus on DTI. Journal of the Neurological Sciences, 2010, 299, 92-96.	0.6	24
46	Example dataset for the hMRI toolbox. Data in Brief, 2019, 25, 104132.	1.0	24
47	Structure predicts function: Combining non-invasive electrophysiology with in-vivo histology. NeuroImage, 2015, 108, 377-385.	4.2	23
48	Pattern and progression of white-matter changes in a case of posterior cortical atrophy using diffusion tensor imaging. Journal of Neurology, Neurosurgery and Psychiatry, 2008, 80, 432-436.	1.9	22
49	High-resolution diffusion kurtosis imaging at 3T enabled by advanced post-processing. Frontiers in Neuroscience, 2014, 8, 427.	2.8	22
50	Hyperelastic Susceptibility Artifact Correction of DTI in SPM. Informatik Aktuell, 2013, , 344-349.	0.6	21
51	Longitudinal changes of spinal cord grey and white matter following spinal cord injury. Journal of Neurology, Neurosurgery and Psychiatry, 2021, 92, 1222-1230.	1.9	20
52	Individual white matter fractional anisotropy analysis on patients with MRI negative partial epilepsy. Journal of Neurology, Neurosurgery and Psychiatry, 2010, 81, 136-139.	1.9	18
53	Local striatal reward signals can be predicted from corticostriatal connectivity. NeuroImage, 2017, 159, 9-17.	4.2	15
54	Interhemispheric Dissociation of Language Regions in a Healthy Subject. Archives of Neurology, 2006, 63, 1344.	4.5	14

#	Article	IF	CITATIONS
55	Progression of microstructural putamen alterations in a case of symptomatic recurrent seizures using diffusion tensor imaging. Seizure: the Journal of the British Epilepsy Association, 2012, 21, 478-481.	2.0	12
56	POAS4SPM: A Toolbox for SPM to Denoise Diffusion MRI Data. Neuroinformatics, 2015, 13, 19-29.	2.8	12
57	Grasping multiple sclerosis: do quantitative motor assessments provide a link between structure and function?. Journal of Neurology, 2013, 260, 407-414.	3.6	10
58	Biophysically motivated efficient estimation of the spatially isotropic component from a single gradientâ€recalled echo measurement. Magnetic Resonance in Medicine, 2019, 82, 1804-1811.	3.0	10
59	Diffusion tensor imaging in a case of Kearns–Sayre syndrome: Striking brainstem involvement as a possible cause of oculomotor symptoms. Journal of the Neurological Sciences, 2009, 281, 110-112.	0.6	9
60	Finding the best clearing approach - Towards 3D wide-scale multimodal imaging of aged human brain tissue. NeuroImage, 2022, 247, 118832.	4.2	7
61	Confinement-induced depletion of the enhancedg-factor in quantum wires. Physical Review B, 2005, 72, ·	3.2	6
62	The Influence of Radio-Frequency Transmit Field Inhomogeneities on the Accuracy of G-ratio Weighted Imaging. Frontiers in Neuroscience, 2021, 15, 674719.	2.8	5
63	Reducing Susceptibility Distortion Related Image Blurring in Diffusion MRI EPI Data. Frontiers in Neuroscience, 2021, 15, 706473.	2.8	5
64	Deficits in tongue motor control are linked to microstructural brain damage in multiple sclerosis: a pilot study. BMC Neurology, 2015, 15, 190.	1.8	4
65	A new method for joint susceptibility artefact correction and super-resolution for dMRI. , 2014, , .		2
66	Towards a representative reference for MRI-based human axon radius assessment using light microscopy. Neurolmage, 2022, 249, 118906.	4.2	2
67	Diffusion tensor imaging demonstrates fiber impairment in Susac's syndrome. Journal of the Neurological Sciences, 2009, 283, 254.	0.6	0